Received: 11 February 2025 | Revised: 15 April 2025 | Accepted: 25 April 2025

DOI: 10.1111/jace.20634

Journal of the American Ceramic Society

SPECIAL ISSUE ARTICLE

Silazane-based zinc-filled coating system for corrosion protection of steel in humid and salt water containing environments

Jan-Felix Wendel[1] | **Nicole Matthée**[2] | **Stefan Schafföner**[1] | **Günter Motz**[1]

[1]Chair of Ceramic Materials Engineering, University of Bayreuth, Bayreuth, Germany

[2]Dörken Coatings GmbH & Co. KG, Herdecke, Germany

Correspondence
Günter Motz, Chair of Ceramic Materials Engineering, University of Bayreuth, Bayreuth 95447, Germany.
Email: guenter.motz@uni-bayreuth.de

Abstract

In this study, a lamellar corrosion protection coating filled with zinc, zinc–magnesium, and aluminum flakes using the polymer-derived ceramic route is developed. The goal is to investigate the potential of polysilazanes as matrix material for zinc-filled base coats providing enhanced temperature stability. Therefore, emphasis is placed on the investigation of the influence of the treatment temperature on the microstructure of the coating using scanning electron microscopy and X-ray diffraction as well as on the mechanical properties using scratch tests. Additionally, the effect of different filler compositions on the protection properties is studied. The best corrosion protection in 5 wt.% sodium chloride solution is attained with a zinc content of 37.5 vol.%, a magnesium content of 30 vol.%, and an aluminum content of 12.5 vol.%. The coating system exhibits improved temperature stability up to 400°C. At higher temperatures the oxidation of the zinc and the zinc–magnesium fillers leads to a severe reduction in corrosion protection. The scratch resistance is not affected by the thermal treatment.

KEYWORDS

corrosion protection, lamellar Zn–Mg–Al coatings, preceramic polymer-derived coatings, saltwater corrosion

1 | INTRODUCTION

Corrosion protection of alloys is a topic of constantly growing importance. In addition to the monetary aspect of having less material damage and longer service life, which is in the range of billions of dollars per country and year,[1,2] corrosion protection enhances the reliability of components and systems preventing damages to humans and the environment. One of the most effective and common strategies to protect metals from the corrosion in salt water are coatings on the basis of zinc. Such coatings offer a cathodic protection to steel components due to the ignoble character of zinc in comparison to iron. This is accompanied by the advantage that zinc is able to provide its protection over a certain local distance, so even regions where the coating is damaged or scratched are still protected. Zinc coatings are often applied as metallic coatings via galvanization. These corrosion protection coatings are widely investigated in many studies. The protection performance of such

coatings can be enhanced by the addition of several alloying elements such as magnesium,[3–9] aluminum,[3,4,8–12] or nickel.[13–15] An extension of the lifetime of more than 300% depending on the corrosion setup and the composition of the alloy has been reported.[6,7,9,16] Disadvantages of such an application process are the emergence of harmful gases and the possibility of hydrogen embrittlement of steel substrates.[17–21] An alternative to the galvanization process is the application of coatings, in which zinc is present as a filler embedded in an organic or inorganic matrix,[22–28] so-called zinc-rich coatings. Especially lamellar coatings are favored due to the barrier effect of the flakes,[29–31] which slows down diffusion of electrolyte through the coating and hence provides improved protection. Zinc-rich coatings are applied by spraying or dipping processes where no hydrogen is formed and impairment of the steel by hydrogen embrittlement is avoided. Further advantages of zinc-rich coatings are the simple control of the application process, the possibility to repair the coatings and that the duration of protection can be easily tailored by the thickness and composition. In the field of automotive components, lamellar zinc coatings are used to protect springs, brake, and chassis components as well as fastening elements.[32–35] Moreover, the agricultural, aviation, and renewable energy sectors are further fields of application with increasing importance.

The most common matrix material for zinc-rich coatings are epoxy resins.[30,31,36–38] They offer a very good adhesion to metals and are stable in corrosive environments,[38,39] but limit the application temperature of the coatings to a maximum of 250°C due to thermal decomposition of the epoxy matrix.[40] Furthermore, high extents of fillers are necessary to ensure electroconductivity between the filler particles and with the substrate.[26,31] In general, a high amount of fillers in an organic polymer matrix makes such zinc-filled coatings susceptible to mechanical loads like scratching or abrasion.[25,27,31,41]

To overcome these problems polysilazanes could be a suitable alternative matrix material. Polysilazanes are preceramic polymers that also offer high chemical stability, which is necessary to withstand the corrosive environments over long periods of time.[42–45] Additionally, they have excellent adhesion to metal surfaces due to the formation of covalent bonds.[46,47] Polymer and ceramic coatings based on polysilazanes can be prepared of up to 100 µm in thickness by spraying using the polymer-derived ceramic technique.[48,49] The properties of the coatings can easily be modified by the addition of a variety of fillers.[49,50] During a thermal treatment usually at temperatures higher than 500°C in a furnace, the silazanes are transformed into a ceramic material leading to an increase in the mechanical properties.[51] Therefore, unlike epoxy resins, elevated temperatures do not cause a loss of mechanical properties or decomposition of the matrix, but could enhance the mechanical properties of the coatings. Furthermore, polysilazanes can reduce the oxidation of the zinc particles at elevated temperatures.

However, the usage of polysilazanes as matrix material could cause some problems. One problem could arise through the electrically insulating character of the polymers. Due to the high affinity of polysilazanes to metals, zinc particles might be coated leading to an impairment of the electrical contacts between them, which are essential for the cathodic protection.

In this study, the development of lamellar zinc-based corrosion protection coatings with polysilazanes as matrix material is presented. The goal was to figure out the potential of the coatings regarding temperature stability, mechanical properties, and corrosion protection of the steel substrates. The study focused on the influence of the thermal treatment on the microstructure and the corrosion protection of the coatings. Additionally, in order to improve the protective properties, the effect of different fillers (Al and Mg) and their contents was investigated.

2 | MATERIALS AND METHODS

All used materials are commercially available. The steel 1.7335 (13CrMo4-5, HSM Stahl- und Metallhandel GmbH) was chosen as substrate due to its widely industrial use, for example, for apparatus construction and its comparatively low intrinsic corrosion resistance. Sheets with a thickness of 2 mm were cut in the dimensions of 70 mm × 30 mm. To remove the oxide layer on the surface of the sheets, sandblasting was used followed by cleaning with acetone in an ultrasonic bath for 20 min and drying. The composition of the steel is given in Table 1.

For all coating systems the silazane precursor Durazane 1800 (Merck KGaA) was selected because of its high chemical resistance, its good adhesion to metals, and its commercial availability. As anticorrosive fillers zinc flakes ProFLAKE Zn 1400, zinc–magnesium flakes STAPA 15 ZnMg26 with 26 wt.% of magnesium (both from ECKART GmbH) and aluminum flakes APS 11 micron (Alfa Aesar GmbH & Co. KG) were used. The particle size distribution of the filler materials was analyzed with a particle size analyzer (PSA 1190, Anton Paar GmbH). The preparation of the coating slurry started with the dissolution of the dispersant (DISPERBYK 2151, Byk-Chemie GmbH) in di-*n*-butylether (>99%, Acros Organics) before the zinc flakes, zinc–magnesium flakes, and aluminum flakes were added. Afterwards a mixture of Durazane 1800 and 3 wt.% of the crosslinking initiator dicumyl peroxide (Sigma–Aldrich GmbH) was added.

The coatings were applied on both sides of the substrates with a semiautomatic spraying device equipped with a

TABLE 1 Chemical composition of the steel 1.7335.

Element	C	Si	Mn	P	S	N	Cu	Cr	Mo	Fe
Min (wt.%)	0.08	–	0.40	–	–	–	–	0.70	0.40	Bal.
Max (wt.%)	0.18	0.35	1.00	0.025	0.010	0.012	0.30	1.15	0.60	Bal.

spray nozzle (model 780S, Nordson EFD) followed by a temperature treatment in a chamber furnace (N 60-HR, Nabertherm GmbH) at 250°C for 1 h in air with a heating rate of 3 K/min. This treatment was chosen to ensure a sufficient crosslinking of the precursor[49,52] and to avoid thermal stressing of the fillers and the substrate material. To test the high temperature stability of the coatings, further treatments were carried out up to 500°C.

To evaluate the microstructure of the coatings, a scanning electron microscope (Gemini Sigma 300VP, Carl Zeiss AG) equipped with an energy-dispersive X-ray spectroscopy (EDS) detector (Octane Super, EDAX, AMETEK GmbH) was used. The acceleration voltage was 10–15 keV and the working distance 8.5 mm. Scratch resistance tests were performed with a scratch hardness tester (Lineartester Model 249, ERICHSEN GmbH & Co. KG) with a moving stylus according to DIN ISO 1518 (Ø 1 mm, scratch speed 35 mm/s) at constant loads. The scratches were evaluated with a digital microscope (DSX 1000, EVIDENT Europe GmbH).

During the development of the coating system an easy and quickly applicable corrosion test was used to characterize the corrosion protection performance of the coatings with different filler compositions (according to standard DIN 50905-4). Therefore, a 35 mm long artificial scratch was applied to the coated samples and they were subsequently exposed to a non-stirring aqueous 5 wt.% sodium chloride (NaCl) solution for 840 h at room temperature. The samples were placed in a 50° angle to the horizontal and the solution was renewed every 168 h (1 week).

After studying the compositions, a selected coating system was investigated regarding its corrosion protection performance by the neutral salt spray (NSS) test and the continuous condensation test (CCT) performed according to the standards DIN EN ISO 9227[53] and DIN EN ISO 6270-1[54] by Dörken Coatings GmbH & Co. KG. For these tests, coated samples in the size of 100 mm × 100 mm were covered at the backside as well as at the cut edges with a protective adhesive tape and epoxy resin, respectively. A perpendicular scratch of 1 mm width and 50 mm length was applied on the coating before the test. The salt spray test was performed at a temperature of 35°C and continuous spraying of an aqueous 5% NaCl solution, whereas the CCT was conducted at 40°C at 100% relative humidity. Three samples were analyzed in each test.

To identify the corrosion products on the surface of the samples and to analyze the coatings phase compositions, X-ray diffraction (XRD) measurements (D8 Discover, Bruker Corporation) in Bragg-Brentano geometry with Cu Kα radiation in the 2θ range of 10°–90° were performed. A step size of 0.02° and a time per step of 0.4 s were chosen.

3 | RESULTS AND DISCUSSION

3.1 | Characterization of the filler materials

As mentioned before, the coatings contain zinc, magnesium, and aluminum as active anticorrosion fillers. It is well known that the different fillers and their amount have an effect on the corrosion protection behavior. Zinc is the main component because of its ability to cathodically protect iron. Magnesium and aluminum enhance the corrosion protection of the coating system in chloride containing environments.[55–57] All metal fillers are ignoble and have a low electrochemical potential. When magnesium and aluminum are used in combination with zinc, the formation of non-soluble corrosion products like Simonkolleite[58–62] or layered double hydroxides (LDHs)[5,60,63–65] (such as zinc aluminum carbonate hydroxides) is observed. These corrosion products can form dense and protective layers on the surface of the samples. The exact mechanism of action has not been fully explained. There are various assumptions given in the literature.[6,9,59,66] From electrochemical impedance spectroscopy measurements, it was concluded that Simonkolleite suppresses the oxygen reduction reaction by blocking the cathodic reaction sites.[63,67] Furthermore, it was suggested that Simonkolleite is stabilized in the presence of magnesium.[6,9,63,67] In general, it can inhibit diffusion by forming dense and non-soluble layers. LDHs also form very stable and dense layers that shield the corrosive medium and inhibit diffusion.[60,68–71] However, most authors agree that these layers of corrosion products are the reason for the improved corrosion protection.

The metallic fillers were examined with regard to their particle size distribution (Table 2) and crystal phase composition (Figure 1).

The zinc and the zinc–magnesium flakes had similar particle size distribution while the aluminum flakes were slightly smaller. The XRD analysis of all fillers showed only peaks corresponding to their respective crystal phases. The pattern of the zinc–magnesium flakes showed

TABLE 2 Particle size distribution of the metallic fillers.

Distribution value	Zn flakes (ProFLAKE Zn 1400)	ZnMg flakes (STAPA 15 ZnMg26)	Al flakes (APS 11 micron)
D10 (μm)	8.9	6.6	2.1
D50 (μm)	16.4	14.3	7.5
D90 (μm)	24.6	25.1	18.3

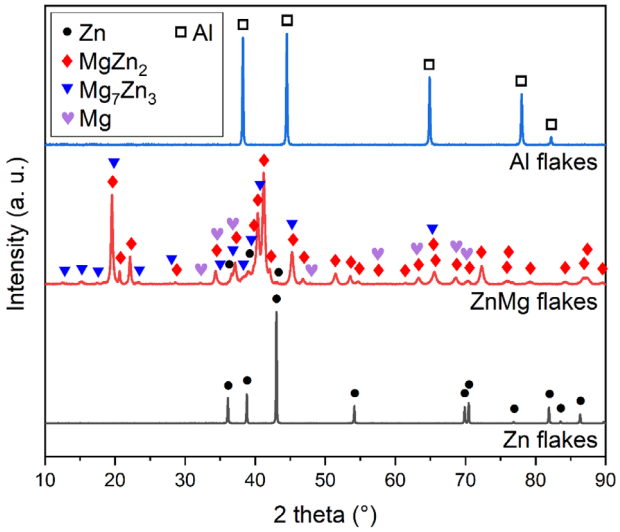

FIGURE 1 X-ray diffraction (XRD) analysis of the metallic fillers Zn, ZnMg, and Al.

predominantly the presence of the $MgZn_2$ phase. Some less intense peaks were attributed to Zn, Mg, and Mg_7Zn_3. The $MgZn_2$ phase is known to provide a good corrosion protection performance.[66]

3.2 | Investigation of the coating composition

To obtain a sacrificial corrosion protection, the metallic fillers need to form an electrically conductive interconnected network and an electrically conductive connection to the substrate. Therefore, the total volume fraction of fillers needs to be sufficiently high to prevent an insulation of the filler particles by the non-conductive matrix material. However, as the filler content increases, the cohesion of the coating components decreases due to reduced availability of binder to maintain the cohesion among filler particles. Therefore, it was first necessary to determine the optimal filler/Durazane 1800 ratio. As a result, the cohesion of the coating cannot be maintained with a filler content of more than 85 vol.% relative to the total coating volume, while a content of less than 50 vol.% avoids the formation of an electrically conductive network. Therefore, a total amount of 80 vol.% of all fillers was used for all coatings prepared in this study to ensure mechanical cohesion of the coatings and to provide sufficient electrical connection between the filler particles.

TABLE 3 Compositions of the Zn–Mg–Al–Durazane 1800 corrosion protection coatings with varying magnesium content.

Coating system	Z1	Z2	Z3
Zinc content (vol.%)	45	37.5	30
Magnesium content (vol.%)	20	30	40
Aluminum content (vol.%)	15	12.5	10
Durazane 1800 (vol.%)	20	20	20

In order to optimize the corrosion protection properties and to study the influence of the individual proportions of fillers, the content of the respective filler was varied. Samples coated with three different compositions of 20, 30, and 40 vol.% of magnesium and constant volume ratio between zinc and aluminum of about 3:1 (Table 3) were prepared (according to the procedure described above) and exposed to 5 wt.% NaCl solution for 840 h. Images of the corroded samples are shown in Figure 2. The samples were qualitatively evaluated with regard to the following criteria: formation of red rust and white rust at the surface, protection of the sample edges, and protection of the scratched region.

As shown in Figure 2, the corrosion protection performance of the coatings differed with varying magnesium content. For the magnesium content of 20 vol.% (system Z1), only a small amount of red rust was noted, while white rust was observed throughout the entire surface. White rust is a typical corrosion product of zinc. At the edges no corrosion damage was visible, but the formation of red rust started in the scratch. With increasing magnesium content (systems Z2 and Z3), the formation of white rust was prevented so almost no corrosion damage was visible at the surface. However, the protection of the edges decreased and the resulting amount of red rust increased with the magnesium content. It is noteworthy to mention that the origin of a corrosion site appeared preferentially at the edge of the samples and grew further toward the middle of the sample. In the sample with 30 vol.% of magnesium (system Z2), the scratch was free of red rust whereas some red rust was detected in the 40 vol.% sample (system Z3).

The lack of white rust at higher magnesium contents than 20 vol.% shows that a certain amount of magnesium is necessary to suppress the formation of white rust. The increase in magnesium content was correlated with a decrease in zinc content with zinc being the filler responsible for long-distance protection. Therefore, the protection of the edges was negatively affected because these regions were under particular corrosion attack. This led to an increased formation of red rust at higher magnesium contents starting from the edges of the samples. On the basis of these results, a magnesium content of 30 vol.% (coating system Z2 with 37.5 vol.% zinc, 30 vol.% magnesium, and

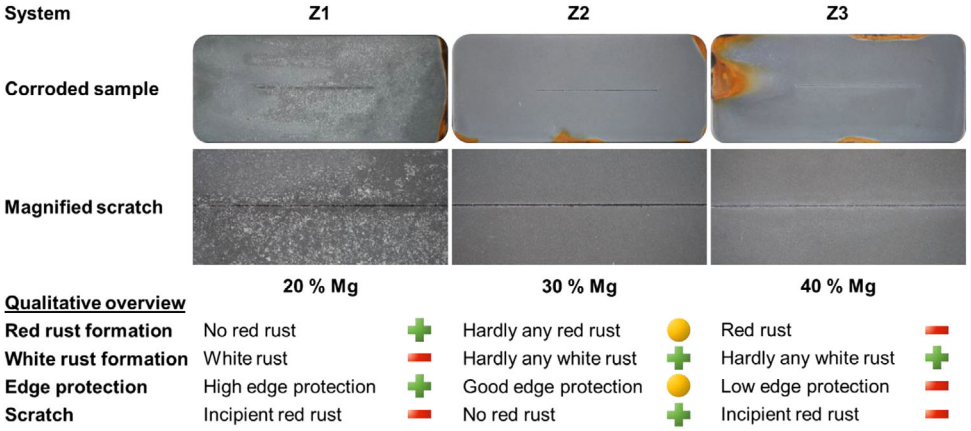

FIGURE 2 Optical images of the scratched Zn–Mg–Al–Durazane 1800 coated steel 1.7335 samples with varying magnesium content treated at 250°C for 1 h in air and corroded in 5 wt.% aqueous NaCl solution for 840 h as well as a qualitative evaluation of the samples.

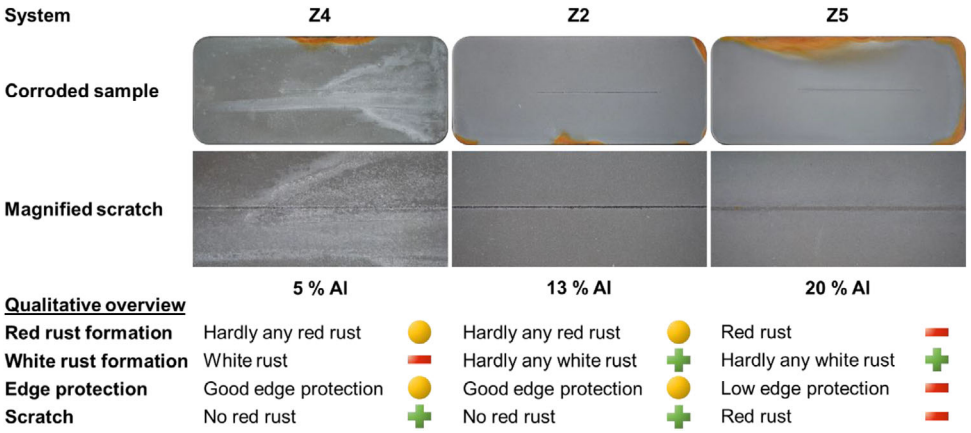

FIGURE 3 Optical images of the scratched Zn–Mg–Al–Durazane 1800 coated steel 1.7335 samples with varying aluminum content treated at 250°C for 1 h in air and corroded in 5 wt.% aqueous NaCl solution for 840 h as well as a qualitative evaluation of the samples.

TABLE 4 Compositions of the Zn–Mg–Al–Durazane 1800 corrosion protection coatings with varying aluminum content.

Coating system	Z4	Z2	Z5
Zinc content (vol.%)	45	37.5	30
Magnesium content (vol.%)	30	30	30
Aluminum content (vol.%)	5	12.5	20
Durazane 1800 (vol.%)	20	20	20

12.5 vol.% aluminum) was the best composition to avoid the formation of red and white rust and therefore selected for further investigations.

To understand the effect of the aluminum content on the corrosion protection properties of the coating system based on Z2, the volume fraction of aluminum was varied between 5 and 20 vol.%. The compositions of the coatings are given in Table 4. The samples were tested under the same conditions as described before. Figure 3 shows the optical images of the corroded samples.

The reduction of the aluminum content (system Z4) compared to coating system Z2 went along with an increase of zinc content. This led to the formation of white rust at the surface of the sample. Furthermore, red rust appeared at the edge of the sample. In the scratch, white rust was observed as the main corrosion product. The overall protection behavior of the coating was comparable to the protection effect of system Z2. An increase of the aluminum content to 20 vol.% (system Z5) led to a very strong formation of red rust at the sample edge and in the scratch. The increase went along with a reduction of the total amount of zinc in the coating. Therefore, the protection of the edges and the overall performance of the coating decreased significantly. Obviously, no white rust formed in this system.

Due to the formation of white rust in coating system Z4 and the strong formation of red rust in system Z5 an aluminum content of 13 vol.% (system Z2) seemed to be an optimum to provide a good corrosion protection.

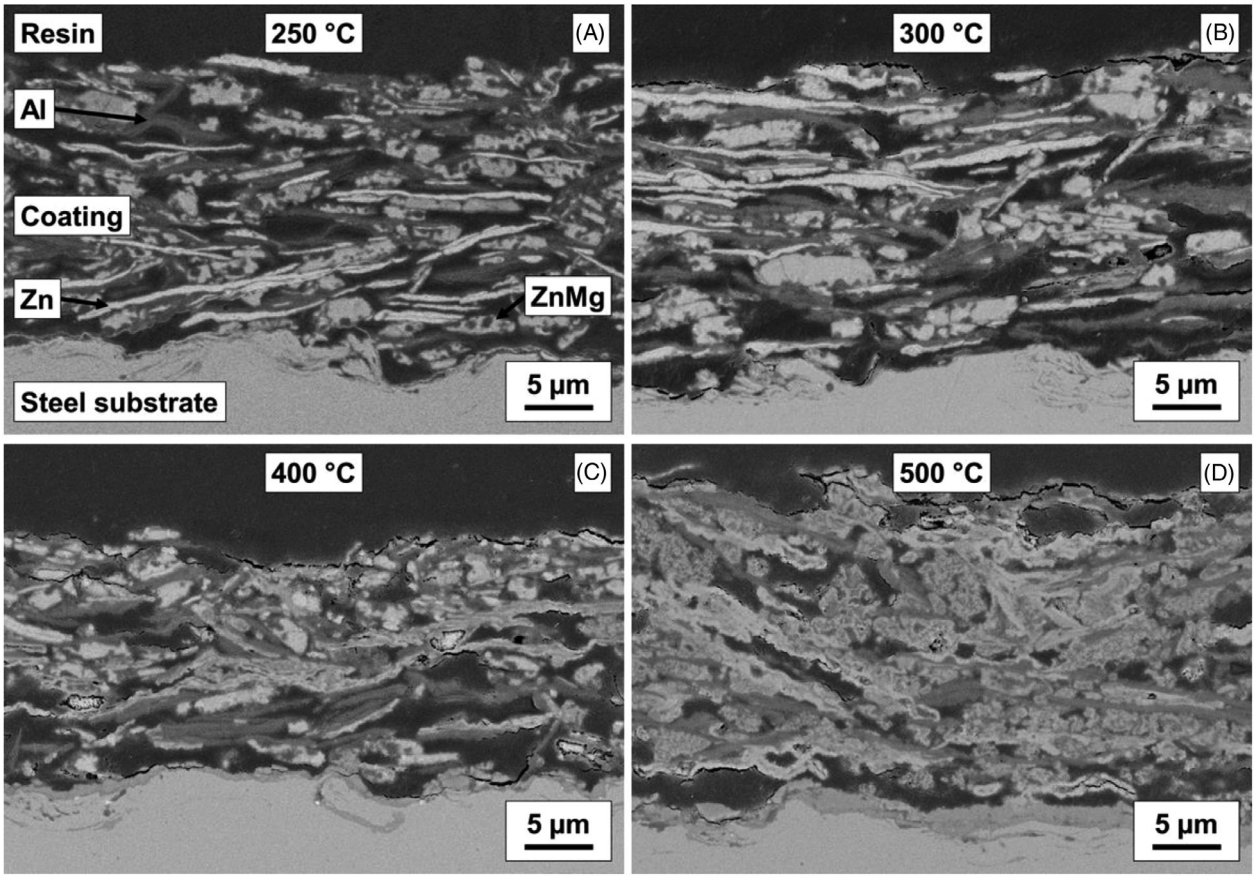

FIGURE 4 Scanning electron microscopy (SEM) cross-sectional images of steel 1.7335 samples coated with composition Z2 treated at (A) 250°C, (B) 300°C, (C) 400°C, and (D) 500°C for 1 h in air.

Therefore, no further modifications of coating system Z2 were necessary.

3.3 | Effects of the thermal treatment on the coating system Z2

The silazane was used as matrix material to increase the temperature stability of the coating system. The treatment temperature influences the coating system in several aspects such as coating thickness, porosity, and formed phases. Initially, the influence of the treatment temperature on the microstructure of coating system Z2 after curing in air between 250°C and 500°C was investigated. Figure 4 shows the SEM cross-sectional images of the microstructure of the respective samples.

The micrographs show a homogeneous distribution of zinc flakes (bright), aluminum flakes (dark), and magnesium flakes (bright with dark spots). At 400°C and more pronounced at 500°C, the zinc and zinc–magnesium flakes began to lose their shape, as zinc has a melting point of 419°C. However, the aluminum flakes with a melting point of 660°C retained their shape

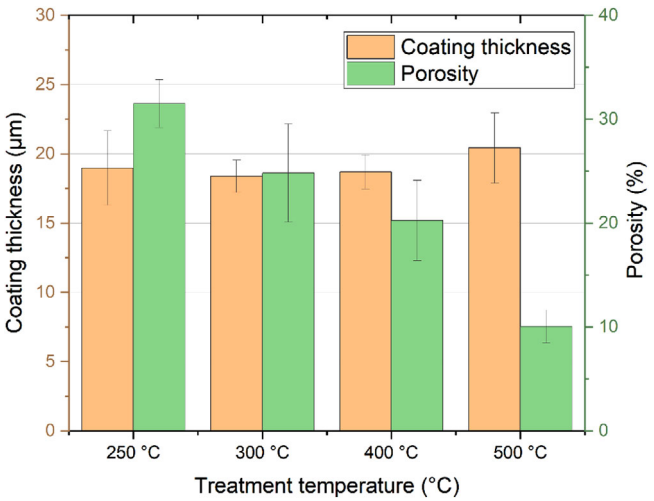

FIGURE 5 Coating thickness and porosity of the coating system Z2 at different treatment temperatures in air.

and stabilized the coating. EDS analyses of the coating surfaces (Table 5) indicated a strong oxidation of the zinc particles, which was confirmed by XRD analysis (Figure 6). As depicted in Figure 5, the coating thickness did not significantly change with the treatment

TABLE 5 Energy-dispersive X-ray spectroscopy analyses of the coating surface (system Z2) after treatment at 250°C and 500°C for 1 h in air as well as of the thermally grown oxide (TGO) layer formed during treatment at 500°C for 1 h in air.

Analyzed area	Element (shell)					
	O K	Mg K	Al K	Si K	Fe K	Zn K
Coating surface treated at 250°C						
Atomic %	16.9	19.1	23.7	3.7	–	36.7
Error (%)	9.4	9.1	8.0	10.3	–	4.8
Coating surface treated at 500°C						
Atomic %	34.8	18.1	17.8	3.1	–	26.3
Error (%)	7.7	8.6	7.6	9.3	–	4.5
TGO layer (treated at 500°C)						
Atomic %	35.1	–	2.8	2.3	59.8	–
Error (%)	6.4	–	11.1	10.3	2.9	–

temperature, but the porosity decreased continuously from about 31% at 250°C to 10% at 500°C. The change in the porosity as a function of the treatment temperature was investigated by the evaluation of several SEM images with the software ImageJ and the trainable Weka segmentation tool. The porosity of about 31% is related to the high content of fillers of 80 vol.%. The decrease of the porosity can be explained by the oxidation of zinc causing an increase in volume. This effect predominates the shrinkage of the precursor with increasing treatment temperature, resulting in a constant layer thickness.

Moreover, the formation of a thermally grown oxide (TGO) layer between the substrate and the coating was detected at 400°C and 500°C. The TGO layer formed by the oxidation of the surface of the steel substrate and, according to the EDS analysis (Table 5), consisted mainly of iron oxide. The layer can disrupt the electrically conductive connection between the coating and the substrate and therefore inhibit the protection of the substrate in the event of a corrosive attack, which has a negative effect on the corrosion protection performance.

To gain information about the changes in phase composition related to the melting of the zinc containing fillers, XRD analyses at all curing temperatures were performed (Figure 6). After treatments at 250°C and 300°C the peaks related to zinc and aluminum and two different Mg–Zn phases ($MgZn_2$ and $Mg_{21}Zn_{25}$) were detected. The latter was not found in the initial analysis of the magnesium flakes (Figure 1). After a treatment at 400°C the peaks of the $Mg_{21}Zn_{25}$ phase disappeared because of its thermal stability up to about 350°C.[72,73] The formation of zinc oxide and zinc magnesium oxide, whose peak positions are similar, was proven. At 500°C, the peaks of the $MgZn_2$ phase also disappeared while the peaks of zinc oxide and zinc magnesium oxide occurred with increased intensity. Additionally, magnesium oxide was detected. The aforementioned results were in accordance with the findings

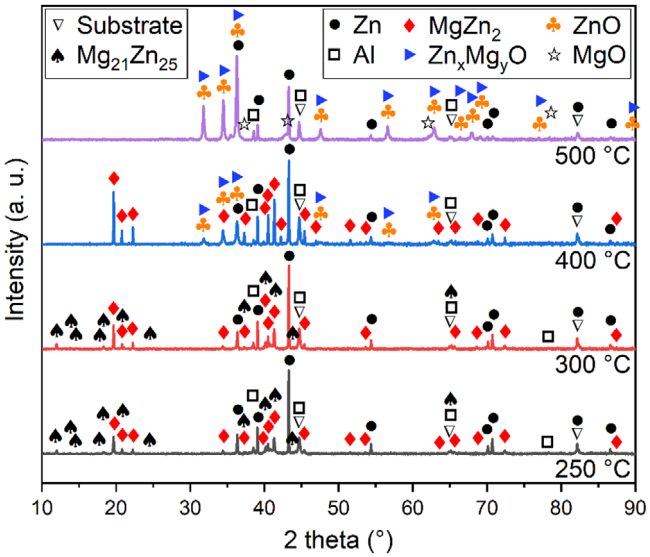

FIGURE 6 X-ray diffraction (XRD) analyses of the coating system Z2 after thermal treatment up to 500°C for 1 h in air.

from the microstructure analysis. In Figure 4d, a melting of the zinc and zinc magnesium phases was observed as well as the formation of zinc oxide indicated by the EDS analysis. The latter is favored by the high reactivity of zinc with oxygen at elevated temperatures[74] whereby the porosity of the coating enabled the oxygen access. The formation of zinc oxide is accompanied by an increase in volume, which contributed to the reduction in porosity. The formed zinc oxide cannot participate in the cathodic protection of the substrate leading to a decreased corrosion protection of the coating system. This was subsequently validated by the immersion corrosion test conducted in aqueous 5 wt.% NaCl solution for 504 h. In Figure 7b, the sample treated at 400°C showed white rust at the scratch and across the surface, which was not seen at lower treatment temperatures. The corrosion protection of the sample treated at 500°C (Figure 7c) was significantly

FIGURE 7 Optical images of scratched samples coated with system Z2 on steel 1.7335 treated at (A) 300°C, (B) 400°C, and (C) 500°C for 1 h in air and corroded in 5 wt.% NaCl solution for 504 h.

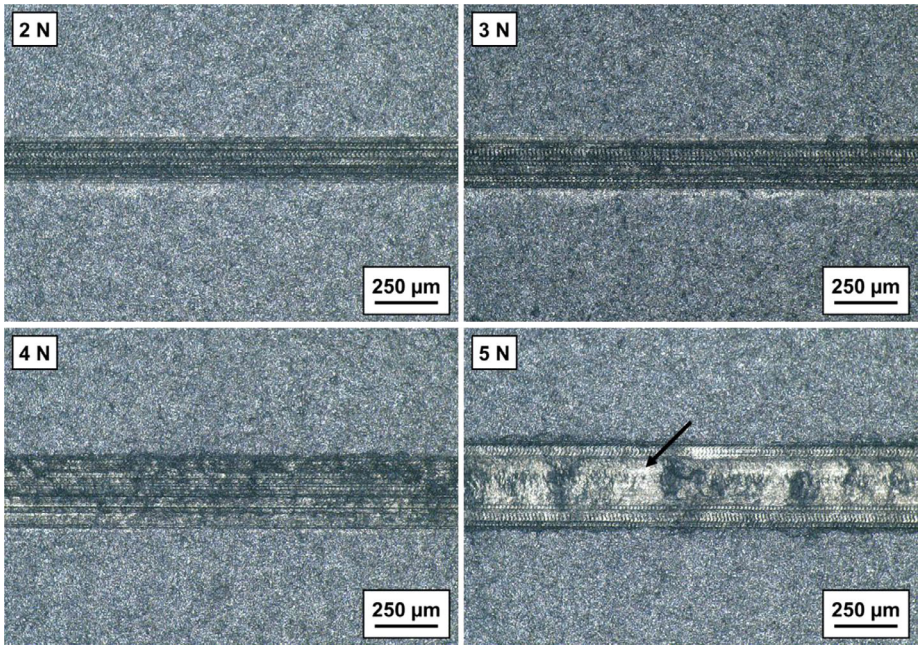

FIGURE 8 Digital microscopy images of scratched samples with coating system Z2 on steel 1.7335 treated at 250°C for 1 h in air.

reduced. Red rust covered the scratch and zinc oxide was visually visible as white patina on the surface. This result demonstrates that the coating system retains a good corrosion resistance for curing temperatures up to 400°C.

3.4 | Scratch resistance

For the mechanical characterization of the coating system Z2, scratch tests were performed with forces up to 5 N after treatment at 250°C (Figure 8) and 500°C (Figure 9).

As is clearly visible, the coating system treated at 250°C (Figure 8) was already scratched at 2 N. With increasing force, the width of the scratches increased, which means a deeper penetration of the stylus into the coating. At 5 N, parts of the substrate were revealed (Figure 8: exposed area of the substrate is marked with an arrow). The low scratch resistance resulted from the porosity of the coating which is related to the high content of lamellar fillers. Additionally, the fillers and the polymeric precursor themselves are soft contributing to a low scratch resistance. After the treatment at 500°C (Figure 9), the scratch width also increased with the force but in contrast to Figure 8 fragments of the coating were visible next to the scratch indicating a more brittle behavior. While some substrate area was revealed at 4 N, even less area was exposed at 5 N compared to the treatment at 250°C. The brittle behavior was a consequence of the beginning transformation of the silazane into a ceramic material and the reduced porosity of the coating. Therefore, higher treatment temperatures resulted in a shift from ductile to brittle behavior, but did not lead to a significant improvement of the mechanical properties. It is not possible to compare these values with other lamellar zinc-based coating systems because of a lack of information in literature. No studies addressing the scratch resistance of lamellar zinc coatings are published yet to the best of our knowledge. Nevertheless, these results demonstrated the vulnerability of the Zn–Mg–Al coating against scratching.

3.5 | Evaluation of the corrosion protection

The corrosion protection of the coating system Z2 was evaluated by the NSS test and CCT according to the

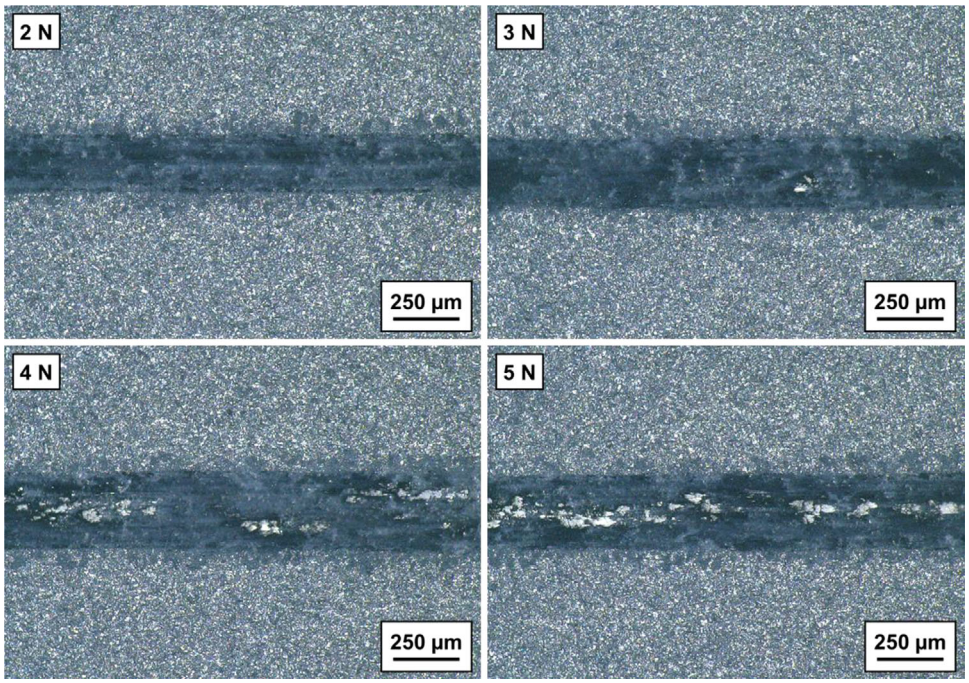

FIGURE 9 Digital microscopy images of scratched samples with coating system Z2 on steel 1.7335 treated at 500°C for 1 h in air.

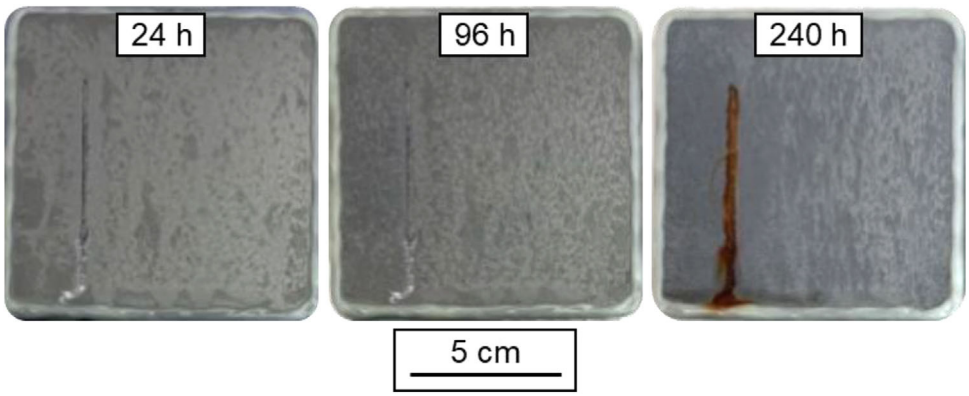

FIGURE 10 Representative optical images of coating system Z2 on steel 1.7335 substrates after corrosion for 24, 96, and 240 h in the neutral salt spray test.

standards DIN EN ISO 9227 and DIN EN ISO 6270-1. For the tests, the coating system treated at 250°C was chosen because it showed the best corrosion protection in the immersion test conducted in 5 wt.% NaCl (Figures 2 and 3). The images of corroded samples during the NSS test are given in Figure 10. White rust was formed in the scratch after 96 h. Subsequently, red rust covered the entire scratch after 192 h, and the test was stopped after 240 h. No red rust formed on the surface of the samples. The XRD analysis of the corrosion products (Figure 11) revealed the formation of Simonkolleite ($Zn_5(OH)_8Cl_2{\cdot}H_2O$, zinc chloride hydroxide hydrate) and a zinc aluminum carbonate hydroxide hydrate from the class of LDHs ($Zn_{0.65}Al_{0.35}(CO_3)_{0.175}(OH)_2{\cdot}(H_2O)_{0.69}$). The exact composition of the LDH was not verified, as the diffractograms of zinc aluminum carbonate hydroxide hydrates with slight differences in stoichiometry hardly differ from each other. Additionally, iron(III) oxide hydroxide was found in the scratch, which is a typical component of red rust. Simonkolleite and the LDH corrosion product are found in serval publications addressing zinc-based coatings in salt spray tests.[9,56,59,60,75,76] Both are insoluble in water and therefore are able to form protective layers on the surface of the coating system which slow down or inhibit further corrosion.[5,58–64] Such a layer is clearly visible in the SEM image (Figure 11). Therefore, the formation of an insoluble layer composed of the corrosion products is proposed to be an important protection mechanism of the

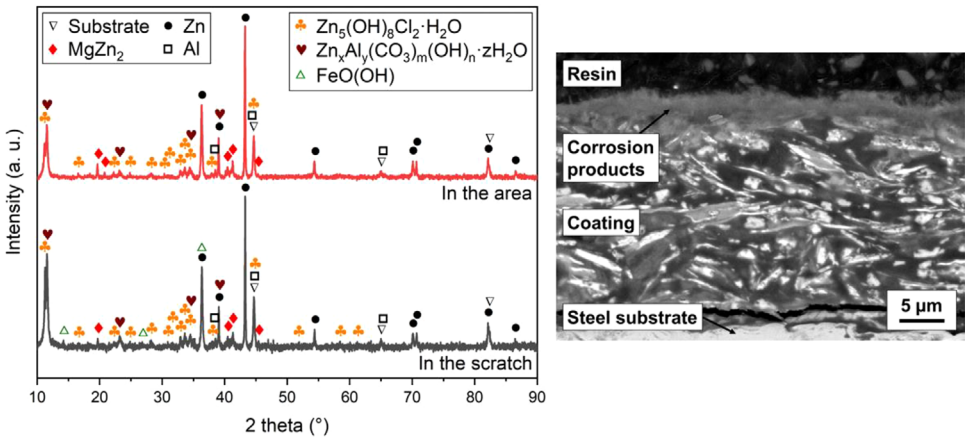

FIGURE 11 X-ray diffraction (XRD) analysis of the corrosion products and scanning electron microscopy (SEM) image of the microstructure of corroded coating system Z2 on steel 1.7335 substrates in the neutral salt spray test after 240 h.

coating system. The fact that Simonkolleite and LDH are the only corrosion products detected, supports the thesis that these corrosion products are stabilized in the presence of magnesium.[9,63,69,77]

Feldmann et al.[27] investigated the corrosion behavior of lamellar zinc coatings on S235JR metal sheets in salt spray tests according to DIN EN ISO 9227. The coatings with a thickness of 9–11 µm contained zinc, aluminum, and zinc–aluminum–magnesium flakes, filled to an amount of about 80 wt.% in an inorganic titanate and silicate matrix. They reported that after a duration of 1000 h in the NSS, the scratched coating system, composed of a mixture of all three types of flakes, exhibited slight white rust formation in the scratch but neither white rust nor red rust formed on the surface. A detailed investigation of the corrosion products on the surface was not carried out. However, this coating system exhibits obviously better corrosion protection in NSS compared to the Z2 coating system developed in this study. There are various reasons for the difference in the protection behavior. As Zubielewicz et al.[31] and Sørensen et al.[39] stated, the corrosion protection behavior is influenced by the amount, size, shape, and composition of the fillers as well as the porosity of the coating. While Feldmann et al. used zinc–aluminum–magnesium flakes, in this work zinc–magnesium flakes were chosen. Other important parameters include the influence of the matrix material and the porosity of the coatings. The silazane-based matrix used in this study is electrically insulating, which could impair the formation of the electrically conductive network between the filler particles. This network is necessary for a cathodic protection mechanism. Additionally, the relatively high porosity of about 30% might have negatively affected the conductive network and the formation of a protective corrosion product layer on the surface, leading to a reduction in corrosion protection. A direct comparison with other organic or inorganic zinc-filled coating systems is difficult because most of the published systems have a significantly higher coating thickness. Kakaei et al.[78] and Zhang et al.[79] prepared inorganic coatings with spherical zinc particles of 70 and 90 µm thickness, respectively, and achieved protection for 1000 h in salt spray test. Zhang et al.[80] studied an epoxy-based coating system with zinc–aluminum–magnesium flakes, which had a thickness of 120 ± 10 µm. They observed red rust after 336 h of salt spray testing. Jagtap et al.[81] reported an epoxy-based lamellar zinc coating system with a thickness of about 70 µm that lasted 1500 h before first signs of corrosion appeared. Vilche et al.[30] also published findings on epoxy-based lamellar coating systems with thicknesses varying from 40 to 80 µm. After 2500 h of salt spray testing, they achieved the best results with minimal corrosion (according to ASTM D 1654-92) using the thickest system. An epoxy-based coating system with spherical zinc particles was investigated by Hayatdavoudi and Rahsepar.[82] The 110 µm thick coating showed red rust in the scratch and on the surface after 1000 h of salt spray testing, though the timing of the first occurrence was not mentioned. Qi et al.[83] reported about an epoxy-based coating with a thickness of 80 ± 10 µm, which showed red rust after 25 days of exposure.

The behavior of the coating system Z2 in a corrosive environment without salt was additionally investigated using the CCT. After 240 h of treatment, first signs of corrosion were visible as small white rust spots on the surface of the samples. No additional corrosion occurred until 696 h. The test was stopped after 1008 h where only a few red rust spots appeared near the edges of the samples (indicated by an arrow in Figure 12). These spots resulted probably from the imperfect semiautomatic spraying process, which deposited less suspension near the side edges than in the center, leading to poorer corrosion protection due to the reduced coating thickness. Magnesium hydroxide

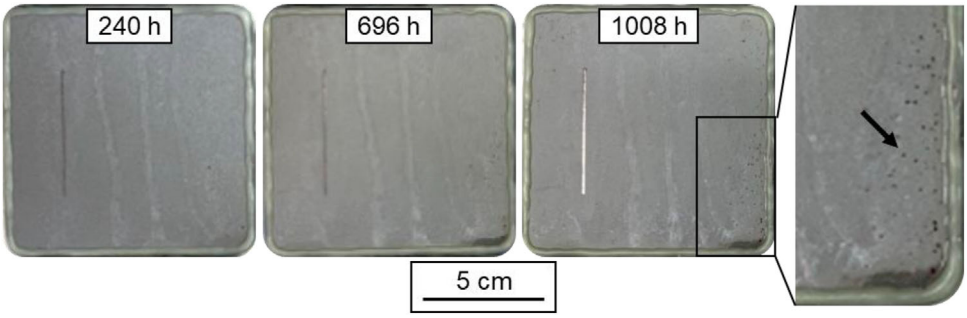

FIGURE 12 Representative optical images of coating system Z2 on steel 1.7335 substrates after corrosion for 240, 696, and 1008 h in the continuous condensation test.

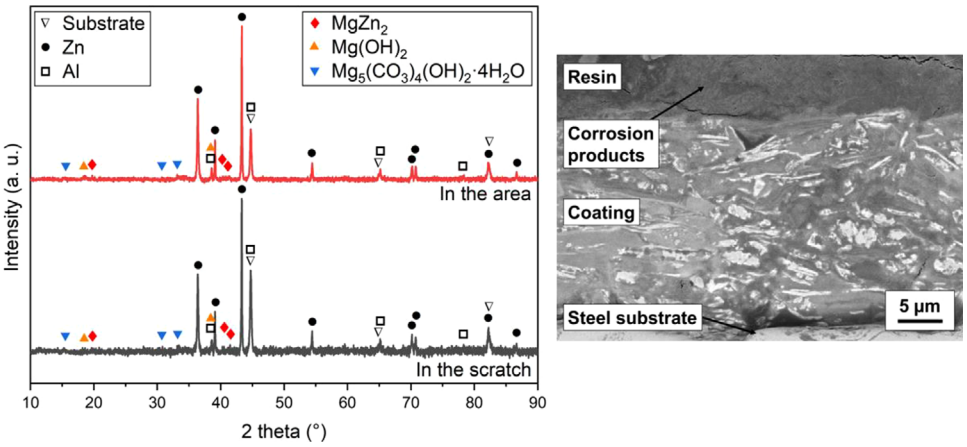

FIGURE 13 X-ray diffraction (XRD) analysis of the corrosion products and scanning electron microscopy (SEM) image of the microstructure of corroded coating system Z2 on steel 1.7335 substrates in the continuous condensation test after 1008 h.

($Mg(OH)_2$) and hydromagnesite ($Mg_5(CO_3)_4(OH)_2{\cdot}4H_2O$, hydrated magnesium hydroxy carbonate) were identified as corrosion products by XRD and SEM/EDS analysis (Figure 13). Magnesium hydroxide is a typical corrosion product of magnesium and zinc containing coatings attributed to the higher reactivity of magnesium compared to zinc, which causes the zinc–magnesium phases to be preferentially attacked.[5,26,63,84,85] Hydromagnesite is formed from magnesium hydroxide in the presence of carbon dioxide.[86–89] Lindström et al.[86] studied the corrosion of magnesium alloys in environments with and without chloride and carbon dioxide and reported lower corrosion rates in the presence of the carbonates compared to pure magnesium hydroxide, concluding higher protective effect. Feliu et al.[89] investigated the corrosion of magnesium alloys in continuous condensation conditions and ascribed the reduced corrosion to the blocking of active corrosion sites by carbonates. The protective properties of magnesium corrosion products are affirmed by the results of this study. In contrast to the NSS test, the LDH and Simonkolleite were not detected, which can be attributed to the absence of chloride ions as previously confirmed by Diler et al.[90] and Rodriguez et al.[88] Feldmann et al.[27] tested their aforementioned coating system composed of a mixture of zinc, aluminum, and zinc–aluminum–magnesium flakes in 100% humid atmosphere (according to DIN EN ISO 6270-2) and obtained no visible formation of white rust neither in the scratch nor on the surface after 1000 h of CCT.

The result of our investigations indicate that the formation of protective corrosion products is an important mechanism against corrosion in humid environments. In the presence of chloride, protective LDH and Simonkolleite are formed, while in absence of chloride, magnesium hydroxide and hydromagnesite are the preferred corrosion products.

4 | CONCLUSION

In the present study, a base coat system for the corrosion protection of steel in humid and salt water environments using zinc, zinc–magnesium, and aluminum flakes in combination with a silazane (Durazane 1800) as preceramic polymer matrix was developed. The silazane precursor was selected to increase the temperature stability

of the coating system and the metal flakes were responsible for an active corrosion protection. It was shown that silazanes are suitable matrix materials for the fabrication of zinc-based anticorrosion coatings. The best composition regarding corrosion protection was achieved with 37.5 vol.% zinc, 30 vol.% magnesium, 12.5 vol.% aluminum, and 20 vol.% Durazane 1800 (coating system Z2). The investigation of the influence of the treatment temperature on the microstructure demonstrated that at temperatures exceeding 400°C, the base coat was compromised due to the melting of the zinc containing phases. This along with the oxidation of the zinc and zinc–magnesium fillers led to a reduction in corrosion protection. However, an increase in temperature stability was achieved compared to epoxy resin-based coating systems. Scratch tests exhibited a scratch resistance of about 5 N independent of the treatment temperature.

Corrosion tests under salt spray (240 h) and continuous condensation (1008 h) conditions revealed that the formation of protective corrosion products is an important mechanism enhancing the performance of the coating. The duration of protection in the salt spray test was shorter in comparison to comparable organic or inorganic zinc-filled coatings reported in literature. However, it must be considered that these coatings had a significantly greater thickness. Nevertheless, in the CCT, the protection performance was very good and comparable with other lamellar zinc coatings.

Summarizing, the coating system possessed an increased temperature stability up to 400°C but still suffered from mechanical vulnerability and oxidation especially of the zinc fillers at elevated temperatures. These issues could be solved by the application of an additional top coat protecting the base coat from oxidation and mechanical load.

ACKNOWLEDGMENTS

Open access funding enabled and organized by Projekt DEAL.

CONFLICT OF INTEREST STATEMENT

The authors declare they have no conflicts of interest.

DATA AVAILABILITY STATEMENT

The data that support the findings of this study are available from the corresponding author upon reasonable request.

ORCID

Jan-Felix Wendel https://orcid.org/0000-0002-2959-4303
Stefan Schafföner https://orcid.org/0000-0002-6526-2496
Günter Motz https://orcid.org/0000-0002-8010-068X

REFERENCES

1. Hou B, Li X, Ma X, Du C, Zhang D, Zheng M, et al. The cost of corrosion in China. npj Mater Degrad. 2017;1(1):4.
2. Kruger J. Cost of metallic corrosion. In: Revie RW, editor. Uhlig's corrosion handbook. 2nd ed. New York: John Wiley & Sons, Inc.; 2000. p. 3–10.
3. Ma Z, Ding C, Lu R, Chen Z, Wu G, Zhang J. Effect of Al and Sn on the microstructure, micro-hardness and corrosion properties of Zn–Al–Mg coatings. Mater Today Commun. 2022;33:104892.
4. Liu Q, Cao Y, Chen S, Xu X, Yao M, Fang J, et al. Hot-dip galvanizing process and the influence of metallic elements on composite coatings. J Compos Sci. 2024;8(5):160.
5. Keppert TA, Luckeneder G, Stellnberger K-H, Commenda C, Mori G, Antrekowitsch H. The effect of magnesium on the corrosion of hot-dip galvanized steel in chloride containing environments. Mater Corros. 2014;65(9):871–80.
6. Hosking NC, Ström MA, Shipway PH, Rudd CD. Corrosion resistance of zinc–magnesium coated steel. Corros Sci. 2007;49(9):3669–95.
7. Kawafoku J, Katoh J, Toyama M, Ikeda K, Nishimoto H, Satoh H. Properties of zinc alloy coated steel sheets obtained by continuous vapor deposition pilot-line. SAE Technical Paper 912272. 1991. p. 43–50.
8. LeBozec N, Thierry D, Peltola A, Luxem L, Luckeneder G, Marchiaro G, et al. Corrosion performance of Zn–Mg–Al coated steel in accelerated corrosion tests used in the automotive industry and field exposures. Mater Corros. 2013;64(11):969–78.
9. Tsujimura T, Komatsu A, Andoh A. Influence of Mg content in coating layer and coating structure on corrosion resistance of hot-dip Zn–Al–Mg alloy coated steel sheet. In: Lamberights M, editor. Zinc and zinc alloy coated steel sheet, Galvatech 2001. Düsseldorf: Stahleisen; 2001. p. 145–52.
10. Panossian Z, Mariaca L, Morcillo M, Flores S, Rocha J, Peña JJ, et al. Steel cathodic protection afforded by zinc, aluminium and zinc/aluminium alloy coatings in the atmosphere. Surf Coat Technol. 2005;190(2–3):244–48.
11. Porter FC, Stoneman AM, Thilthorpe RG. The range of zinc coatings. Trans IMF. 1988;66(1):28–33.
12. Büteführ M. Zinc–aluminium-coatings as corrosion protection for steel. Mater Corros. 2007;58(9):721–26.
13. Short NR, Abibsi A, Dennis JK. Corrosion resistance of electroplated zinc alloy coatings. Trans IMF. 1989;67(1):73–77.
14. Miura N, Saito T, Kanamura T, Shindo Y, Kitazawa Y. Development of new corrosion-resistant steel sheets for automobiles. Trans ISIJ. 1983;23(11):913–22.
15. Porter FC. Zinc handbook: properties, processing, and use in design. New York: Dekker; 1991.
16. Morishita M, Koyama K, Murase M, Mori Y. Improvement in the corrosion resistance of zinc-plated steel by electrodeposition of magnesium from a molten salt. ISIJ Int. 1996;36(6):714–19.
17. Pinger T, Riedel J, Diehl A, Mayrhofer R. Investigation of the hydrogen embrittlement susceptibility of steel components during thin-film hot-dip galvanizing. Mater Test. 2022;64(5):667–77.
18. Hillier E, Robinson MJ. Hydrogen embrittlement of high strength steel electroplated with zinc–cobalt alloys. Corros Sci. 2004;46(3):715–27.

19. Rehrl J. Wasserstoffversprödung in hochfesten, mikrolegierten Stählen. Dissertation. München: Technische Universität München; 2014. 186 p.
20. Borchers C, Michler T, Pundt A. Effect of hydrogen on the mechanical properties of stainless steels. Adv Eng Mater. 2008;10(1–2):11–23.
21. Shreyas P, Panda B, Vishwanatha AD. Embrittlement of hot-dip galvanized steel: a review. In: M Satyanarayana Gupta, TVK Gupta, N Kishore Nath, editors. 3rd International Conference on "Advancements in Aeromechanical Materials for Manufacturing". Vol. 020038. AIP Publishing; 2021.
22. Xing C, Wang W, Qu S, Tang Y, Zhao X, Zuo Y. Degradation of zinc-rich epoxy coating in 3.5% NaCl solution and evolution of its EIS parameters. J Coat Technol Res. 2021;18(3):843–60.
23. Zhang W, Xia W, Chen Z, Zhang G, Qian S, Lin Z. Comparison of the cathodic protection of epoxy resin coating/zinc-rich coatings on defective areas under atmospheric and immersion conditions: the secondary activation of zinc particles. Coatings. 2024;14(3):336.
24. Hoang N, Khoa TA, Le Nhung T, Phuong PM, Binh TD, Hang TTX, et al. Flake ZnAl alloy as an effective pigment in silicate coatings for the corrosion protection of steel. Coatings. 2022;12(8):1046.
25. Langer E, Zubielewicz M, Królikowska A, Komorowski L, Krawczyk K, Wanner M, et al. Zinc-reduced anticorrosive primers—water-based versus solvent-based. Coatings. 2025;15(1):64.
26. Plagemann P, Weise J, Zockoll A. Zinc–magnesium-pigment rich coatings for corrosion protection of aluminum alloys. Prog Org Coat. 2013;76(4):616–25.
27. Feldmann F, Mears LLE, Roth M, Valtiner M. Characterisation of the galvanic protection of zinc flake coating by spectroelectrochemistry and industrial testing. Mater Corros. 2023;74(8):1148–58.
28. Gergely A, Pászti Z, Bertóti I, Mihály J, Drotár E, Török T. Hybrid zinc-rich paint coatings: the impact of incorporation of nano-size inhibitor and electrical conducting particles. In: Tiwari A, Rawlins J, Hihara LH, editors. Intelligent coatings for corrosion control. Boston: Butterworth-Heinemann; 2015. p. 195–249.
29. Kalendová A. Effects of particle sizes and shapes of zinc metal on the properties of anticorrosive coatings. Prog Org Coat. 2003;46(4):324–32.
30. Vilche JR, Bucharsky EC, Giudice CA. Application of EIS and SEM to evaluate the influence of pigment shape and content in ZRP formulations on the corrosion prevention of naval steel. Corros Sci. 2002;44(6):1287–309.
31. Zubielewicz M, Langer E, Królikowska A, Komorowski L, Wanner M, Krawczyk K, et al. Concepts of steel protection by coatings with a reduced content of zinc pigments. Prog Org Coat. 2021;161:106471.
32. Dörken MKS-Systeme GmbH & Co. KG. Coating chassis parts correctly. Int Surf Technol. 2019;12(1):16–17.
33. Dörken MKS-Systeme GmbH & Co. KG. Reliable corrosion protection for wheel hubs. Int Surf Technol. 2019;12(4):18–19.
34. Fackiner A. A focus on tension. Int Surf Technol. 2015;8(2):28–29.
35. Knott R, Schneider J. Rigorously implemented. JOT. 2012;5(2):42–43.
36. Marchebois H, Touzain S, Joiret S, Bernard J, Savall C. Zinc-rich powder coatings corrosion in sea water: influence of conductive pigments. Prog Org Coat. 2002;45(4):415–21.
37. Li HY, Duan JY, Wei DD. Comparison on corrosion behaviour of arc sprayed and zinc-rich coatings. Surf Coat Technol. 2013;235:259–66.
38. Hussain AK, Seetharamaiah N, Pichumani M, Chakra CS. Research progress in organic zinc rich primer coatings for cathodic protection of metals—a comprehensive review. Prog Org Coat. 2021;153:106040.
39. Sørensen PA, Kiil S, Dam-Johansen K, Weinell CE. Anticorrosive coatings: a review. J Coat Technol Res. 2009;6(2):135–76.
40. Chatterjee A. Thermal degradation analysis of thermoset resins. J Appl Polym Sci. 2009;114(3):1417–25.
41. Schaefer K, Miszczyk A. Improvement of electrochemical action of zinc-rich paints by addition of nanoparticulate zinc. Corros Sci. 2013;66:380–91.
42. Li C, Wei J, Chen M, Guan X, Yang X, Li Z, et al. Ultralow-temperature fabrication of chromium-free zinc-aluminum coatings based on polysilazane. Mater Chem Phys. 2022;278:125608.
43. Rossi S, Deflorian F, Fedel M. Polysilazane-based coatings: corrosion protection and anti-graffiti properties. Surf Eng. 2019;35(4):343–50.
44. Choi HJ, Lu K. Polysilazane-derived SiON coating on stainless steel weld for corrosion resistance. Mater Chem Phys. 2024;315:128988.
45. Fedel M, Rodríguez Gómez FJ, Rossi S, Deflorian F. Characterization of polyorganosilazane-derived hybrid coatings for the corrosion protection of mild steel in chloride solution. Coatings. 2019;9(10):680.
46. Amouzou D, Fourdrinier L, Maseri F, Sporken R. Formation of me—O–Si covalent bonds at the interface between polysilazane and stainless steel. Appl Surf Sci. 2014;320:519–23.
47. Günthner M, Kraus T, Dierdorf A, Decker D, Krenkel W, Motz G. Advanced coatings on the basis of Si(C)N precursors for protection of steel against oxidation. J Eur Ceram Soc. 2009;29(10):2061–68.
48. Günthner M, Schütz A, Glatzel U, Wang K, Bordia RK, Greißl O, et al. High performance environmental barrier coatings. Part I: passive filler loaded SiCN system for steel. J Eur Ceram Soc. 2011;31(15):3003–10.
49. Barroso G, Li Q, Bordia RK, Motz G. Polymeric and ceramic silicon-based coatings—a review. J Mater Chem A. 2019;7(5):1936–63.
50. Colombo P, Mera G, Riedel R, Sorarù GD. Polymer-derived ceramics: 40 years of research and innovation in advanced ceramics. J Am Ceram Soc. 2010;93(7):1805–37.
51. Günthner M, Wang K, Bordia RK, Motz G. Conversion behaviour and resulting mechanical properties of polysilazane-based coatings. J Eur Ceram Soc. 2012;32(9):1883–92.
52. Barroso GS, Krenkel W, Motz G. Low thermal conductivity coating system for application up to 1000°C by simple PDC processing with active and passive fillers. J Eur Ceram Soc. 2015;35(12):3339–48.
53. Corrosion tests in artificial atmospheres - Salt spray tests (ISO 9227:2022); German version EN ISO 9227:2022;77.060(9227). Berlin: Beuth Verlag GmbH; 2022.
54. Paints and varnishes - Determination of resistance to humidity - Part 1: Condensation (single-sided exposure) (ISO 6270-1:2017);

German version EN ISO 6270-1:2018;87.040(6270-1). Berlin: Beuth Verlag GmbH; 2018.
55. Odnevall Wallinder I, Leygraf C. A critical review on corrosion and runoff from zinc and zinc-based alloys in atmospheric environments. Corrosion. 2017;73(9):1060–77.
56. Schürz S, Luckeneder GH, Fleischanderl M, Mack P, Gsaller H, Kneissl AC, et al. Chemistry of corrosion products on Zn–Al–Mg alloy coated steel. Corros Sci. 2010;52(10):3271–79.
57. Guttmann H, Belisle S, Esson DG. Galfan—a new coating for automotive tubing. SAE Trans. 1986;95:185–90.
58. Ishikawa T, Ueda M, Kandori K, Nakayama T. Air permeability of the artificially synthesized Zn–Al–Mg alloy rusts. Corros Sci. 2007;49(6):2547–56.
59. Schuerz S, Fleischanderl M, Luckeneder GH, Preis K, Haunschmied T, Mori G, et al. Corrosion behaviour of Zn–Al–Mg coated steel sheet in sodium chloride-containing environment. Corros Sci. 2009;51(10):2355–63.
60. Volovitch P, Vu TN, Allély C, Abdel Aal A, Ogle K. Understanding corrosion via corrosion product characterization: II. Role of alloying elements in improving the corrosion resistance of Zn–Al–Mg coatings on steel. Corros Sci. 2011;53(8):2437–45.
61. LeBozec N, Thierry D, Rohwerder M, Persson D, Luckeneder G, Luxem L. Effect of carbon dioxide on the atmospheric corrosion of Zn–Mg–Al coated steel. Corros Sci. 2013;74:379–86.
62. Ishikawa T, Matsumoto K, Yasukawa A, Kandori K, Nakayama T, Tsubota T. Influence of metal ions on the formation of artificial zinc rusts. Corros Sci. 2004;46(2):329–42.
63. Salgueiro Azevedo M, Allély C, Ogle K, Volovitch P. Corrosion mechanisms of Zn(Mg,Al) coated steel: 2. The effect of Mg and Al alloying on the formation and properties of corrosion products in different electrolytes. Corros Sci. 2015;90:482–90.
64. Persson D, Thierry D, LeBozec N, Prosek T. In situ infrared reflection spectroscopy studies of the initial atmospheric corrosion of Zn–Al–Mg coated steel. Corros Sci. 2013;72:54–63.
65. Boidot A, Gheno F, Bentiss F, Jama C, Vogt J-B. Effect of aluminum flakes on corrosion protection behavior of water-based hybrid zinc-rich coatings for carbon steel substrate in NaCl environment. Coatings. 2022;12(10):1390.
66. Prosek T, Nazarov A, Bexell U, Thierry D, Serak J. Corrosion mechanism of model zinc–magnesium alloys in atmospheric conditions. Corros Sci. 2008;50(8):2216–31.
67. Rai PK, Rout D, Satish Kumar D, Sharma S, Balachandran G. Effect of magnesium on corrosion behavior of hot-dip Zn–Al–Mg coating. J Mater Eng Perform. 2021;30(6):4138–47.
68. Liu W, Li Q, Li M-C. Corrosion behaviour of hot-dip Al–Zn–Si and Al–Zn–Si–3Mg coatings in NaCl solution. Corros Sci. 2017;121:72–83.
69. Amanian S, Naderi R, Mahdavian M. The role of an in-situ grown Zn–Al layered double hydroxide conversion coating in the protective properties of epoxy coating on galvanized steel. J Electrochem Soc. 2022;169(3):031511.
70. Holzner T, Luckeneder G, Strauß B, Valtiner M. Environmentally friendly layered double hydroxide conversion layers: formation kinetics on Zn–Al–Mg-coated steel. ACS Appl Mater Interfaces. 2022;14(4):6109–19.
71. Yang Y, Wang Y, Huang Q, Zhao J, Gao F, Wei Y. Effect of ZnAl-LDH on corrosion resistance of Zn–55Al alloy in NaCl solution. Mater Corros. 2023;74(10):1439–55.
72. Okamoto H. Comment on Mg–Zn (magnesium–zinc). J Phase Equilib. 1994;15(1):129–30.
73. Okamoto H. Supplemental literature review of binary phase diagrams: Cs–In, Cs–K, Cs–Rb, Eu–In, Ho–Mn, K–Rb, Li–Mg, Mg–Nd, Mg–Zn, Mn–Sm, O–Sb, and Si–Sr. J Phase Equilib Diffus. 2013;34(3):251–63.
74. Hammer GE, Shemenski RM. The oxidation of zinc in air studied by XPS and AES. J Vac Sci Technol A. 1983;1(2):1026–28.
75. Prosek T, Hagström J, Persson D, Fuertes N, Lindberg F, Chocholatý O, et al. Effect of the microstructure of Zn–Al and Zn–Al–Mg model alloys on corrosion stability. Corros Sci. 2016;110:71–81.
76. Salgueiro Azevedo M, Allély C, Ogle K, Volovitch P. Corrosion mechanisms of Zn(Mg, Al) coated steel in accelerated tests and natural exposure: 1. The role of electrolyte composition in the nature of corrosion products and relative corrosion rate. Corros Sci. 2015;90:472–81.
77. Liu W, Li M-C, Luo Q, Fan H-Q, Zhang J-Y, Lu H-S, et al. Influence of alloyed magnesium on the microstructure and long-term corrosion behavior of hot-dip Al–Zn–Si coating in NaCl solution. Corros Sci. 2016;104:217–26.
78. Kakaei MN, Danaee I, Zaarei D. Investigation of corrosion protection afforded by inorganic anticorrosive coatings comprising micaceous iron oxide and zinc dust. Corros Eng Sci Technol. 2013;48(3):194–98.
79. Zhang C, Liu B, Li S, Zhang Z, Wu B, Emori W, et al. Effects of the particle size distribution of zinc powder on the anticorrosion performance of water-borne inorganic zinc-rich coatings. Corros Eng Sci Technol. 2024;60(1):13–25.
80. Zhang J, Zhu Q, Wang Z, Wang X, Yan J. Flake-like ZnAl alloy powder modified waterborne epoxy coatings with enhanced corrosion resistance. Prog Org Coat. 2023;175:107367.
81. Jagtap RN, Patil PP, Hassan SZ. Effect of zinc oxide in combating corrosion in zinc-rich primer. Prog Org Coat. 2008;63(4):389–94.
82. Hayatdavoudi H, Rahsepar M. Smart inhibition action of layered double hydroxide nanocontainers in zinc-rich epoxy coating for active corrosion protection of carbon steel substrate. J Alloys Compd. 2017;711:560–67.
83. Qi C, Weinell CE, Dam-Johansen K, Wu H. Assessment of anticorrosion performance of zinc-rich epoxy coatings added with zinc fibers for corrosion protection of steel. ACS Omega. 2023;8(2):1912–22.
84. Makar GL, Kruger J. Corrosion of magnesium. Int Mater Rev. 1993;38(3):138–53.
85. Sullivan J, Mehraban S, Elvins J. In situ monitoring of the microstructural corrosion mechanisms of zinc–magnesium–aluminium alloys using time lapse microscopy. Corros Sci. 2011;53(6):2208–15.
86. Lindström R, Johansson L-G, Svensson J-E. The influence of NaCl and CO_2 on the atmospheric corrosion of magnesium alloy AZ91. Mater Corros. 2003;54(8):587–94.
87. Lindström R, Johansson L-G, Thompson GE, Skeldon P, Svensson J-E. Corrosion of magnesium in humid air. Corros Sci. 2004;46(5):1141–58.

88. Rodriguez J, Chenoy L, Roobroeck A, Godet S, Olivier M-G. Effect of the electrolyte pH on the corrosion mechanisms of Zn–Mg coated steel. Corros Sci. 2016;108:47–59.
89. Feliu Jr. S, Maffiotte C, Galván JC, Barranco V. Atmospheric corrosion of magnesium alloys AZ31 and AZ61 under continuous condensation conditions. Corros Sci. 2011;53(5):1865–72.
90. Diler E, Rouvellou B, Rioual S, Lescop B, Nguyen Vien G, Thierry D. Characterization of corrosion products of Zn and Zn–Mg–Al coated steel in a marine atmosphere. Corros Sci. 2014;87:111–17.

How to cite this article: Wendel J-F, Matthée N, Schafföner S, Motz G. Silazane-based zinc-filled coating system for corrosion protection of steel in humid and salt water containing environments. J Am Ceram Soc. 2025;108:e20634. https://doi.org/10.1111/jace.20634